



Search for the standard model Higgs boson produced in association with a Z boson in 7.9 fb^{-1} of $p\bar{p}$ collisions at $\sqrt{s} = 1.96 \text{ TeV}$ using the CDF II detector

CDF Collaboration

T. Aaltonen^a, B. Álvarez González^{b,27}, S. Amerio^c, D. Amidei^e, A. Anastassov^{f,25}, A. Annovi^g, J. Antos^{h,i}, G. Apollinari^f, J.A. Appel^f, T. Arisawa^j, A. Artikov^k, J. Asadi^l, W. Ashmanskas^f, B. Auerbach^m, A. Aurisano^l, F. Azfarⁿ, W. Badgett^f, T. Bae^{o,p,q,r,s,t}, A. Barbaro-Galtieri^u, V.E. Barnes^v, B.A. Barnett^w, P. Barria^z, P. Bartos^{h,i}, M. Baucé^d, F. Bedeschi^x, S. Behari^w, G. Bellettini^y, J. Bellinger^{ab}, D. Benjamin^{ac}, A. Beretvas^f, A. Bhatti^{ad}, D. Bisello^d, I. Bizjak^{ae}, K.R. Bland^{af}, B. Blumenfeld^w, A. Bocci^{ac}, A. Bodek^{ag}, D. Bortoletto^v, J. Boudreau^{ah}, A. Boveia^{ai}, L. Brigliadori^{ak}, C. Bromberg^{al}, E. Brucken^a, J. Budagov^k, H.S. Budd^{ag}, K. Burkett^f, G. Busetto^d, P. Bussey^{am}, A. Buzatu^{an,ao,ap,aq}, A. Calamba^{ar}, C. Calancha^{as}, S. Camarda^{at}, M. Campanelli^{ae}, M. Campbell^e, F. Canelli^{ai,f}, B. Carls^{au}, D. Carlsmith^{ab}, R. Carosi^x, S. Carrillo^{av,14}, S. Carron^f, B. Casal^{b,12}, M. Casarsa^{aw}, A. Castro^{ak}, P. Catastini^{ay}, D. Cauz^{aw}, V. Cavaliere^{au}, M. Cavalli-Sforza^{at}, A. Cerri^{u,7}, L. Cerrito^{ae,20}, Y.C. Chen^{az}, M. Chertok^{ba}, G. Chiarelli^x, G. Chlachidze^f, F. Chlebana^f, K. Cho^{o,p,q,r,s,t}, D. Chokheli^k, W.H. Chung^{ab}, Y.S. Chung^{ag}, M.A. Ciocci^z, A. Clark^{bb}, C. Clarke^{bc}, G. Compostella^d, M.E. Convery^f, J. Conway^{ba}, M. Corbo^f, M. Cordelli^g, C.A. Cox^{ba}, D.J. Cox^{ba}, F. Crescioli^y, J. Cuevas^{b,27}, R. Culbertson^f, D. Dagenhart^f, N. d'Ascenzo^{f,24}, M. Datta^f, P. de Barbaro^{ag}, M. Dell'Orso^y, L. Demortier^{ad}, M. Deninno^{aj}, F. Devoto^a, M. d'Errico^d, A. Di Canto^y, B. Di Ruzza^f, J.R. Dittmann^{af}, M. D'Onofrio^{bd}, S. Donati^y, P. Dong^f, M. Dorigo^{aw}, T. Dorigo^c, K. Ebina^j, A. Elagin^l, A. Eppig^e, R. Erbacher^{ba}, S. Errede^{au}, N. Ershaidat^{f,31}, R. Eusebi^l, S. Farringtonⁿ, M. Feindt^{be}, J.P. Fernandez^{as}, R. Field^{av}, G. Flanagan^{f,22}, R. Forrest^{ba}, M.J. Frank^{af}, M. Franklin^{ay}, J.C. Freeman^f, Y. Funakoshi^j, I. Furic^{av}, M. Gallinaro^{ad}, J.E. Garcia^{bb}, A.F. Garfinkel^v, P. Garosi^z, H. Gerberich^{au}, E. Gerchtein^f, S. Giagu^{bf}, V. Giakoumopoulou^{bh}, P. Giannetti^x, K. Gibson^{ah}, C.M. Ginsburg^f, N. Giokaris^{bh}, P. Giromini^g, G. Giurgiu^w, V. Glagolev^k, D. Glenzinski^f, M. Gold^{bi}, D. Goldin^l, N. Goldschmidt^{av}, A. Golossanov^f, G. Gomez^b, G. Gomez-Ceballos^{bj}, M. Goncharov^{bj}, O. González^{as}, I. Gorelov^{bi}, A.T. Goshaw^{ac}, K. Goulianos^{ad}, S. Grinstein^{at}, C. Grosso-Pilcher^{ai}, R.C. Group^{bq,f}, J. Guimaraes da Costa^{ay}, S.R. Hahn^f, E. Halkiadakis^{bk}, A. Hamaguchi^{bl}, J.Y. Han^{ag}, F. Happacher^g, K. Hara^{bm}, D. Hare^{bk}, M. Hare^{bn}, R.F. Harr^{bc}, K. Hatakeyama^{af}, C. Haysⁿ, M. Heck^{be}, J. Heinrich^{bo}, M. Herndon^{ab}, S. Hewamanage^{af}, A. Hocker^f, W. Hopkins^{f,8}, D. Horn^{be}, S. Hou^{az}, R.E. Hughes^{bp}, M. Hurwitz^{ai}, U. Husemann^m, N. Hussain^{an,ao,ap,aq}, M. Hussein^{al}, J. Huston^{al}, G. Introzzi^x, M. Iori^{bg}, A. Ivanov^{ba,17}, E. James^f, D. Jang^{ar}, B. Jayatilaka^{ac}, E.J. Jeon^{o,p,q,r,s,t}, S. Jindariani^f, M. Jones^v, K.K. Joo^{o,p,q,r,s,t}, S.Y. Jun^{ar}, T.R. Junk^f, T. Kamon^{ai,l}, P.E. Karchin^{bc}, A. Kasmi^{af}, Y. Kato^{bl,16}, W. Ketchum^{ai}, J. Keung^{bo}, V. Khotilovich^l, B. Kilminster^f, D.H. Kim^{o,p,q,r,s,t}, H.S. Kim^{o,p,q,r,s,t}, J.E. Kim^{o,p,q,r,s,t}, M.J. Kim^g, S.B. Kim^{o,p,q,r,s,t}, S.H. Kim^{bm}, Y.K. Kim^{ai}, Y.J. Kim^{o,p,q,r,s,t}, N. Kimura^j, M. Kirby^f, S. Klimenko^{av}, K. Knoepfel^f, K. Kondo^{j,1}, D.J. Kong^{o,p,q,r,s,t}, J. Konigsberg^{av}, A.V. Kotwal^{ac}, M. Kreps^{be}, J. Kroll^{bo}, D. Krop^{ai}, M. Kruse^{ac}, V. Krutelyov^{l,4}, T. Kuhr^{be}, M. Kurata^{bm}, S. Kwang^{ai}, A.T. Laasanen^v, S. Lami^x, S. Lammel^f, M. Lancaster^{ae}, R.L. Lander^{ba}, K. Lannon^{bp,26}, A. Lath^{bk}, G. Latino^z, T. LeCompte^{bq}, E. Lee^l, H.S. Lee^{ai,18}, J.S. Lee^{o,p,q,r,s,t}, S.W. Lee^{l,29}, S. Leo^y, S. Leone^x, J.D. Lewis^f, A. Limosani^{ac,21}, C.-J. Lin^u, M. Lindgren^f, E. Lipeles^{bo}, A. Lister^{bb}, D.O. Litvintsev^f, C. Liu^{ah}, H. Liu^{br}, Q. Liu^v, T. Liu^f, S. Lockwitz^m, A. Loginov^m, D. Lucchesi^d, J. Lueck^{be}, P. Lujan^u, P. Lukens^f, G. Lungu^{ad}, J. Lys^u, R. Lysak^{h,i,6}, R. Madrak^f, K. Maeshima^f, P. Maestro^z, S. Malik^{ad},

G. Manca^{bd,2}, A. Manousakis-Katsikakis^{bh}, F. Margaroli^{bf}, C. Marino^{be}, M. Martínez^{at}, P. Mastrandrea^{bf}, K. Matera^{au}, M.E. Mattson^{bc}, A. Mazzacane^f, P. Mazzanti^{aj}, K.S. McFarland^{ag}, P. McIntyre^l, R. McNulty^{bd,11}, A. Mehta^{bd}, P. Mehtala^a, C. Mesropian^{ad}, T. Miao^f, D. Mietlicki^e, A. Mitra^{az}, H. Miyake^{bm}, S. Moed^f, N. Moggi^{aj}, M.N. Mondragon^{f,14}, C.S. Moon^{o,p,q,r,s,t}, R. Moore^f, M.J. Morello^{aa}, J. Morlock^{be}, P. Movilla Fernandez^f, A. Mukherjee^f, Th. Muller^{be}, P. Murat^f, M. Mussini^{ak}, J. Nachtman^{f,15}, Y. Nagai^{bm}, J. Naganoma^j, I. Nakano^{bs}, A. Napier^{bn}, J. Nett^l, C. Neu^{br}, M.S. Neubauer^{au}, J. Nielsen^{u,5}, L. Nodulman^{bq}, S.Y. Noh^{o,p,q,r,s,t}, O. Norniella^{au}, L. Oakesⁿ, S.H. Oh^{ac}, Y.D. Oh^{o,p,q,r,s,t}, I. Oksuzian^{br}, T. Okusawa^{bl}, R. Orava^a, L. Ortolan^{at}, S. Pagan Griso^d, C. Pagliarone^{aw}, E. Palencia^{b,7}, V. Papadimitriou^f, A.A. Paramonov^{bq}, J. Patrick^f, G. Pauletta^{ax}, M. Paulini^{ar}, C. Paus^{bj}, D.E. Pellett^{ba}, A. Penzo^{aw}, T.J. Phillips^{ac}, G. Piacentino^x, E. Pianori^{bo}, J. Pilot^{bp,*}, K. Pitts^{au}, C. Plager^{bt}, L. Pondrom^{ab}, S. Poprocki^{f,8}, K. Potamianos^v, F. Prokoshin^{k,30}, A. Pranko^u, F. Ptohos^{g,9}, G. Punzi^y, A. Rahaman^{ah}, V. Ramakrishnan^{ab}, N. Ranjan^v, I. Redondo^{as}, P. Rentonⁿ, M. Rescigno^{bf}, T. Riddick^{ae}, F. Rimondi^{ak}, L. Ristori^{be,f}, A. Robson^{am}, T. Rodrigo^b, T. Rodriguez^{bo}, E. Rogers^{au}, S. Rolli^{bn,10}, R. Roser^f, F. Ruffini^z, A. Ruiz^b, J. Russ^{ar}, V. Rusu^f, A. Safonov^l, W.K. Sakumoto^{ag}, Y. Sakurai^j, L. Santi^{ax}, K. Sato^{bm}, V. Saveliev^{f,24}, A. Savoy-Navarro^{f,28}, P. Schlabach^f, A. Schmidt^{be}, E.E. Schmidt^f, T. Schwarz^f, L. Scodellaro^b, A. Scribano^z, F. Scuri^x, S. Seidel^{bi}, Y. Seiya^{bl}, A. Semenov^k, F. Sforza^z, S.Z. Shalhout^{ba}, T. Shears^{bd}, P.F. Shepard^{ah}, M. Shimojima^{bm,23}, M. Shochet^{ai}, I. Shreyber-Tecker^{bu}, A. Simonenko^k, P. Sinervo^{an,ao,ap,aq}, K. Sliwa^{bn}, J.R. Smith^{ba}, F.D. Snider^f, A. Soha^f, V. Sorin^{at}, H. Song^{ah}, P. Squillacioti^z, M. Stancari^f, R. St. Denis^{am}, B. Stelzer^{an,ao,ap,aq}, O. Stelzer-Chilton^{an,ao,ap,aq}, D. Stentz^{f,25}, J. Strologas^{bi}, G.L. Strycker^e, Y. Sudo^{bm}, A. Sukhanov^f, I. Suslov^k, K. Takemasa^{bm}, Y. Takeuchi^{bm}, J. Tang^{ai}, M. Tecchio^e, P.K. Teng^{az}, J. Thom^{f,8}, J. Thome^{ar}, G.A. Thompson^{au}, E. Thomson^{bo}, P. Tipton^m, D. Toback^l, S. Tokar^{h,i}, K. Tollefson^{al}, T. Tomura^{bm}, D. Tonelli^f, S. Torre^g, D. Torretta^f, P. Totaro^c, M. Trovato^{aa}, F. Ukegawa^{bm}, S. Uozumi^{o,p,q,r,s,t}, A. Varganov^e, F. Vázquez^{av,14}, G. Velev^f, C. Vellidis^f, M. Vidal^v, I. Vila^b, R. Vilar^b, J. Vizán^b, M. Vogel^{bi}, G. Volpi^g, P. Wagner^{bo}, R.L. Wagner^f, T. Wakisaka^{bl}, R. Wallny^{bt}, S.M. Wang^{az}, A. Warburton^{an,ao,ap,aq}, D. Waters^{ae}, W.C. Wester III^f, D. Whiteson^{bo,3}, A.B. Wicklund^{bq}, E. Wicklund^f, S. Wilbur^{ai}, F. Wick^{be}, H.H. Williams^{bo}, J.S. Wilson^{bp}, P. Wilson^f, B.L. Winer^{bp}, P. Wittich^{f,8}, S. Wolbers^f, H. Wolfe^{bp}, T. Wright^e, X. Wu^{bb}, Z. Wu^{af}, K. Yamamoto^{bl}, D. Yamato^{bl}, T. Yang^f, U.K. Yang^{ai,19}, Y.C. Yang^{o,p,q,r,s,t}, W.-M. Yao^u, G.P. Yeh^f, K. Yi^{f,15}, J. Yoh^f, K. Yorita^j, T. Yoshida^{bl,13}, G.B. Yu^{ac}, I. Yu^{o,p,q,r,s,t}, S.S. Yu^f, J.C. Yun^f, A. Zanetti^{aw}, Y. Zeng^{ac}, C. Zhou^{ac}, S. Zucchelli^{ak}

^a Division of High Energy Physics, Department of Physics, University of Helsinki and Helsinki Institute of Physics, FIN-00014, Helsinki, Finland

^b Instituto de Física de Cantabria, CSIC – University of Cantabria, 39005 Santander, Spain

^c Istituto Nazionale di Fisica Nucleare, Sezione di Padova-Trento, Italy

^d University of Padova, I-35131 Padova, Italy

^e University of Michigan, Ann Arbor, MI 48109, USA

^f Fermi National Accelerator Laboratory, Batavia, IL 60510, USA

^g Laboratori Nazionali di Frascati, Istituto Nazionale di Fisica Nucleare, I-00044 Frascati, Italy

^h Comenius University, 842 48 Bratislava, Slovakia

ⁱ Institute of Experimental Physics, 040 01 Kosice, Slovakia

^j Waseda University, Tokyo 169, Japan

^k Joint Institute for Nuclear Research, RU-141980 Dubna, Russia

^l Texas A&M University, College Station, TX 77843, USA

^m Yale University, New Haven, CT 06520, USA

ⁿ University of Oxford, Oxford OX1 3RH, United Kingdom

^o Center for High Energy Physics, Kyungpook National University, Daegu 702-701, Republic of Korea

^p Seoul National University, Seoul 151-742, Republic of Korea

^q Sungkyunkwan University, Suwon 440-746, Republic of Korea

^r Korea Institute of Science and Technology Information, Daejeon 305-806, Republic of Korea

^s Chonnam National University, Gwangju 500-757, Republic of Korea

^t Chonbuk National University, Jeonju 561-756, Republic of Korea

^u Ernest Orlando Lawrence Berkeley National Laboratory, Berkeley, CA 94720, USA

^v Purdue University, West Lafayette, IN 47907, USA

^w The Johns Hopkins University, Baltimore, MD 21218, USA

^x Istituto Nazionale di Fisica Nucleare Pisa, Pisa, Italy

^y University of Pisa, Pisa, Italy

^z University of Siena, Siena, Italy

^{aa} Scuola Normale Superiore, I-56127 Pisa, Italy

^{ab} University of Wisconsin, Madison, WI 53706, USA

^{ac} Duke University, Durham, NC 27708, USA

^{ad} The Rockefeller University, New York, NY 10065, USA

^{ae} University College London, London WC1E 6BT, United Kingdom

^{af} Baylor University, Waco, TX 76798, USA

^{ag} University of Rochester, Rochester, NY 14627, USA

^{ah} University of Pittsburgh, Pittsburgh, PA 15260, USA

- ^{ai} Enrico Fermi Institute, University of Chicago, Chicago, IL 60637, USA
^{aj} Istituto Nazionale di Fisica Nucleare, Bologna, Italy
^{ak} University of Bologna, I-40127 Bologna, Italy
^{al} Michigan State University, East Lansing, MI 48824, USA
^{am} Glasgow University, Glasgow G12 8QQ, United Kingdom
^{an} Institute of Particle Physics, McGill University, Montréal, Québec, H3A 2T8 Canada
^{ao} Simon Fraser University, Burnaby, British Columbia, V5A 1S6 Canada
^{ap} University of Toronto, Toronto, Ontario, M5S 1A7 Canada
^{aq} TRIUMF, Vancouver, British Columbia, V6T 2A3 Canada
^{ar} Carnegie Mellon University, Pittsburgh, PA 15213, USA
^{as} Centro de Investigaciones Energeticas Medioambientales y Tecnológicas, E-28040 Madrid, Spain
^{at} Institut de Física d'Altes Energies, ICREA, Universitat Autònoma de Barcelona, E-08193 Bellaterra (Barcelona), Spain
^{au} University of Illinois, Urbana, IL 61801, USA
^{av} University of Florida, Gainesville, FL 32611, USA
^{aw} Istituto Nazionale di Fisica Nucleare Trieste/Udine, I-34100 Trieste, Italy
^{ax} University of Udine, I-33100 Udine, Italy
^{ay} Harvard University, Cambridge, MA 02138, USA
^{az} Institute of Physics, Academia Sinica, Taipei, Taiwan 11529, ROC
^{ba} University of California, Davis, Davis, CA 95616, USA
^{bb} University of Geneva, CH-1211 Geneva 4, Switzerland
^{bc} Wayne State University, Detroit, MI 48201, USA
^{bd} University of Liverpool, Liverpool L69 7ZE, United Kingdom
^{be} Institut für Experimentelle Kernphysik, Karlsruhe Institute of Technology, D-76131 Karlsruhe, Germany
^{bf} Istituto Nazionale di Fisica Nucleare, Sezione di Roma 1, Italy
^{bg} Sapienza Università di Roma, I-00185 Roma, Italy
^{bh} University of Athens, 157 71 Athens, Greece
^{bi} University of New Mexico, Albuquerque, NM 87131, USA
^{bj} Massachusetts Institute of Technology, Cambridge, MA 02139, USA
^{bk} Rutgers University, Piscataway, NJ 08855, USA
^{bl} Osaka City University, Osaka 588, Japan
^{bm} University of Tsukuba, Tsukuba, Ibaraki 305, Japan
^{bn} Tufts University, Medford, MA 02155, USA
^{bo} University of Pennsylvania, Philadelphia, PA 19104, USA
^{bp} The Ohio State University, Columbus, OH 43210, USA
^{bq} Argonne National Laboratory, Argonne, IL 60439, USA
^{br} University of Virginia, Charlottesville, VA 22906, USA
^{bs} Okayama University, Okayama 700-8530, Japan
^{bt} University of California, Los Angeles, Los Angeles, CA 90024, USA
^{bu} Institution for Theoretical and Experimental Physics, ITEP, Moscow 117259, Russia

ARTICLE INFO

Article history:

Received 11 June 2012

Received in revised form 11 July 2012

Accepted 20 July 2012

Available online 24 July 2012

Editor: M. Doser

Keywords:

CDF

Higgs boson searches

Multivariate techniques

ABSTRACT

We present a search for the standard model Higgs boson produced in association with a Z boson, using up to 7.9 fb^{-1} of integrated luminosity from $p\bar{p}$ collisions collected with the CDF II detector. We utilize several novel techniques, including multivariate lepton selection, multivariate trigger parametrization, and a multi-stage signal discriminant consisting of specialized functions trained to distinguish individual backgrounds. By increasing acceptance and enhancing signal discrimination, these techniques have significantly improved the sensitivity of the analysis above what was expected from a larger dataset alone. We observe no significant evidence for a signal, and we set limits on the ZH production cross section. For a Higgs boson with mass $115 \text{ GeV}/c^2$, we expect (observe) a limit of 3.9 (4.8) times the standard model predicted value, at the 95% credibility level.

© 2012 Elsevier B.V. Open access under CC BY license.

* Corresponding author.

E-mail address: jrpilot@ucdavis.edu (J. Pilot).¹ Deceased.² Visitor from Istituto Nazionale di Fisica Nucleare, Sezione di Cagliari, 09042 Monserrato (Cagliari), Italy.³ Visitor from University of CA Irvine, Irvine, CA 92697, USA.⁴ Visitor from University of CA Santa Barbara, Santa Barbara, CA 93106, USA.⁵ Visitor from University of CA Santa Cruz, Santa Cruz, CA 95064, USA.⁶ Visitor from Institute of Physics, Academy of Sciences of the Czech Republic, Czech Republic.⁷ Visitor from CERN, CH-1211 Geneva, Switzerland.⁸ Visitor from Cornell University, Ithaca, NY 14853, USA.⁹ Visitor from University of Cyprus, Nicosia CY-1678, Cyprus.¹⁰ Visitor from Office of Science, U.S. Department of Energy, Washington, DC 20585, USA.¹¹ Visitor from University College Dublin, Dublin 4, Ireland.¹² Visitor from ETH, 8092 Zurich, Switzerland.¹³ Visitor from University of Fukui, Fukui City, Fukui Prefecture, 910-0017 Japan.¹⁴ Visitor from Universidad Iberoamericana, Mexico DF, Mexico.¹⁵ Visitor from University of Iowa, Iowa City, IA 52242, USA.¹⁶ Visitor from Kinki University, Higashi-Osaka City, 577-8502 Japan.¹⁷ Visitor from Kansas State University, Manhattan, KS 66506, USA.

1. Introduction

The Higgs boson is the remaining unobserved particle of the standard model (SM) [1–3] predicted by the Higgs mechanism, which is postulated to describe the origin of electroweak symmetry breaking and elementary particle masses. Direct searches at LEP and the Tevatron have excluded SM Higgs bosons with masses (m_H) below $114.4 \text{ GeV}/c^2$ [4] and in the range $156 \leq m_H \leq 177 \text{ GeV}/c^2$ [5], respectively, at the 95% credibility level (CL). Recent results from the ATLAS and CMS experiments [6,7] have extended the excluded range of masses to $127 \leq m_H \leq 600 \text{ GeV}/c^2$ (at the 95% confidence level). ATLAS also excludes Higgs bosons with masses in the range $112.9 \leq m_H \leq 115.5 \text{ GeV}/c^2$ [6].

Production of Higgs bosons at the Tevatron primarily proceeds through the gluon fusion mechanism, $gg \rightarrow H$ [8]. Low-mass Higgs bosons ($m_H < 135 \text{ GeV}/c^2$) decay predominantly to a pair of b quarks, with a branching fraction of 79% (40%) [8] for $m_H = 100$ (135) GeV/c^2 . Due to overwhelming QCD multijet production, low-mass searches with Higgs production via gluon fusion and $H \rightarrow b\bar{b}$ decay are not feasible. To overcome this difficulty, we utilize the associated production of a Higgs boson with a massive vector boson, where leptonic decays of the vector boson produce distinctive event signatures.

This Letter presents a search for the SM Higgs boson using the $ZH \rightarrow \ell^+ \ell^- b\bar{b}$ process, where ℓ is an electron (e) or muon (μ). We search for events containing two oppositely-charged leptons consistent with the decay of a Z boson, and a hadronic signature consistent with the $H \rightarrow b\bar{b}$ decay mode. Previous searches [9,10] by the CDF and D0 Collaborations have demonstrated that this final state provides good sensitivity to a Higgs boson signal, primarily due to the ability of the experiments to reconstruct both the Z and Higgs bosons. We study data from $p\bar{p}$ collisions at $\sqrt{s} = 1.96 \text{ TeV}$ recorded by the CDF II detector. We combine two independent analyses, one with $Z \rightarrow e^+e^-$ [11] and one with $Z \rightarrow \mu^+\mu^-$ [12], using data corresponding to 7.5 and 7.9 fb^{-1} of integrated luminosity, respectively.

The CDF II detector [13] consists of silicon-based and wire-drift-chamber tracking systems immersed in a 1.4 T magnetic field for particle momentum determination. Surrounding the tracking systems are electromagnetic and hadronic calorimeters, providing coverage in the pseudorapidity³² range $|\eta| < 3.6$. Additional drift chambers used for muon identification are located in the outermost layer of the detector.

The sensitivity of this updated analysis is enhanced by using several novel techniques following two general strategies: increasing acceptance and enhancing signal discrimination. To increase acceptance, we introduce artificial neural networks (NNs) for lepton

selection, and we also use several online event-selection (trigger) algorithms not previously used. Using a new technique, we are able to accurately model the combined behavior of these triggers, allowing access to ZH candidate events beyond the reach of the previous CDF searches. To enhance signal discrimination, we form a multi-stage event discriminant organized to isolate ZH candidates from known SM and instrumental processes (backgrounds).

2. Multivariate lepton identification

To improve on standard cut-based lepton identification, we instead select leptons consistent with the decay of a Z boson by using several NNs. Each NN identifies individual electrons or muons, distinguishing them from both non-leptonic candidates and true leptons not originating from Z decays. A single NN is used for muon identification, and is trained [14] to distinguish between true muons from simulated Z decays and misidentified muons from a data sample containing pairs of same-charge muon candidates. The input quantities giving the best discrimination power include the energy deposited by the muon candidate in the calorimeters, the angular separation between the muon candidate and nearest jet, and the number of hits recorded by the tracking systems. In events with $Z \rightarrow \mu\mu$ decays well contained in the detector, the muon NN selection achieves a Z identification efficiency of $\sim 96\%$, while simultaneously rejecting $\sim 94\%$ of the non- Z background. The muon NN selection has increased the signal acceptance for dimuon events by $\sim 10\%$.

Detector geometry [15,16] motivates three NNs for electron identification. One is optimized for identification in the pseudorapidity range $|\eta| < 1.1$, and is trained to distinguish between electrons from simulated events and both jets from collision data along with electrons from data events not considered in this analysis. The other two NNs are trained for the forward regions; one considers only candidates with a silicon-based track and the other considers candidates without such a track in the region $1.1 \leq |\eta| \leq 2.8$. Again, electrons from simulated events are used in the training sample, along with electron candidates from data that may or may not have an associated track. The most discriminating variables in the electron NN include the ratio of the energy deposits in the hadronic and electromagnetic calorimeters, the electron candidate transverse momentum, and shape variables related to the shower formation in the calorimeter. Compared to the selection utilized in previous searches, the electron NN has improved the rejection of jets misidentified as electrons by a factor of five. In total, the multivariate lepton selection has increased the acceptance of the analysis by $\sim 20\%$ over previous searches [9].

3. Event selection

Complementary to the improved lepton identification, we add additional triggers that were not previously utilized in this analysis channel. Rather than using a single trigger with a threshold for muon p_T or electron E_T for the respective Z selection, we consider any event selected by any trigger in three general sets. The first set includes several triggers that select events containing muon detector and drift chamber activity indicative of a high- p_T muon [17,18]. Included in this category may be triggers with lower p_T thresholds than the default muon trigger. The second set of triggers selects events with a large calorimeter-energy imbalance (missing transverse energy, \cancel{E}_T ³³). Some of these events contain muons that

¹⁸ Visitor from Ewha Womans University, Seoul 120-750, Republic of Korea.

¹⁹ Visitor from University of Manchester, Manchester M13 9PL, United Kingdom.

²⁰ Visitor from Queen Mary University of London, London E1 4NS, United Kingdom.

²¹ Visitor from University of Melbourne, Victoria 3010, Australia.

²² Visitor from Muons, Inc., Batavia, IL 60510, USA.

²³ Visitor from Visitor from Nagasaki Institute of Applied Science, Nagasaki, Japan.

²⁴ Visitor from National Research Nuclear University, Moscow, Russia.

²⁵ Visitor from Northwestern University, Evanston, IL 60208, USA.

²⁶ Visitor from University of Notre Dame, Notre Dame, IN 46556, USA.

²⁷ Visitor from Universidad de Oviedo, E-33007 Oviedo, Spain.

²⁸ Visitor from CNRS-IN2P3, Paris, F-75205 France.

²⁹ Visitor from Texas Tech University, Lubbock, TX 79609, USA.

³⁰ Visitor from Universidad Tecnica Federico Santa Maria, 110v Valparaiso, Chile.

³¹ Visitor from Yarmouk University, Irbid 211-63, Jordan.

³² We use a cylindrical coordinate system with z along the proton beam direction, r the perpendicular radius from the central axis of the detector, and ϕ the azimuthal angle. For θ the polar angle from the proton beam, we define $\eta = -\ln \tan(\theta/2)$, transverse momentum $p_T = p \sin \theta$ and transverse energy $E_T = E \sin \theta$.

³³ The missing transverse energy, \cancel{E}_T , is defined by $\vec{\cancel{E}}_T = -\sum_i E_T^i \hat{n}^i$, where i is the number of the calorimeter tower with $|\eta| < 3.6$ and \hat{n}^i is a unit vector perpendicular to the beam axis and pointing at the i th calorimeter tower. We also define $\cancel{E}_T = |\vec{\cancel{E}}_T|$.

are not selected with the high- p_T muon trigger, thereby increasing the acceptance of this analysis. A third set of triggers selects events with activity in the calorimeter suggestive of a high- E_T electron [19]. By using these sets of triggers rather than just single triggers for each lepton type, we increase the event selection acceptance by $\sim 10\%$. To model the complicated correlations between kinematic variables used in the trigger selection described above, we use a novel technique that uses NN functions to parametrize trigger efficiencies as a function of kinematic observables [11,12].

Utilizing the above strategies to increase acceptance, we select events containing opposite-sign,³⁴ same-flavor lepton pairs with $m_{\ell\ell}$ in a window $([76, 106] \text{ GeV}/c^2)$ centered on the mass of the Z boson. Additionally, we require at least two jets [20], with transverse energy $E_T > 25 \text{ GeV}$ for the leading jet, and $E_T > 15 \text{ GeV}$ for all other jets. All jets are required to come from the central region of the detector, $|\eta| < 2.0$.

4. Background composition and signal expectation

We define a pre-tag region (PT) before applying b -quark jet identification, consisting of events with a reconstructed Z boson and two or more jets passing the criteria described above. We observe 33 975 events in the PT region, and expect a total background yield of $34\,200 \pm 4800$ events, where the quoted uncertainty includes both systematic and statistical contributions. We expect 13.6 ± 1.1 ZH signal events in the PT region, for $m_H = 115 \text{ GeV}/c^2$. The dominant process in the PT region is Z + light-flavor (LF) jets (u , d , s , and gluon jets), accounting for $\sim 85\%$ of the total background. Z + heavy-flavor (b and c) jets events, which contribute less than 10% of the background, are a small contribution in the PT region, but become relatively more significant in the signal regions. These processes are modeled using ALPGEN [21] to simulate the hard-scatter process, and PYTHIA [22] for the subsequent hadronization. The Z + jets processes are simulated at leading order and require a K -factor of 1.4 [23] for normalization to NLO cross sections. Other small backgrounds include diboson (ZZ , WZ , and WW) events and $t\bar{t}$ events, simulated entirely with PYTHIA normalized to NLO [24] and NNLO [25] predictions, respectively. Finally, other processes, such as QCD multijet production, can produce two selected leptons in the event. For muon events, this background is modeled using same-charge muon pairs from data. For electron events, we measure the rate of jets passing the electron NN using collision data to estimate the contribution from these processes. This background accounts for $\sim 3\%$ of the background in the PT region.

We utilize two different b -quark-identifying algorithms to search for jets consistent with the $H \rightarrow b\bar{b}$ decay. The secondary vertex algorithm (SV) [26] identifies jets consistent with the decay of a long-lived b hadron by searching for displaced vertices. The SV algorithm has both a tight and a loose operating point – the loose point has better b -jet identification efficiency but also has a higher rate of jets incorrectly identified as b jets. The jet probability (JP) algorithm [27] uses track impact parameters relative to the primary vertex to construct a likelihood for all jet tracks to have originated from the primary vertex. Both algorithms have imperfect rejection of c -quark jets, allowing some events containing them to contribute to the final signal regions.

We use the combination of the two highest- E_T jets to form potential Higgs boson candidates. We use a hierarchy of tag combinations to define three independent signal regions. We first search for events with two tight SV tags – defining the double-tag (DT) region, the most sensitive. A second signal region includes events

Table 1

Expected background and observed data events for the three independent signal regions. Also shown is the expected number of ZH signal events, for a SM Higgs boson with $m_H = 115 \text{ GeV}/c^2$. Quoted uncertainties include both systematic and statistical contributions.

Process	ST	LJP	DT
$Z + \text{LF}, Z + c\bar{c}$	683 ± 65	61 ± 9	7.6 ± 1.2
$Z + b\bar{b}$	287 ± 72	58 ± 15	42 ± 10
$t\bar{t}$	69 ± 7	29 ± 2	26 ± 3
Diboson	42 ± 3	9.5 ± 0.7	6.7 ± 0.6
Other	46 ± 12	3.4 ± 0.3	0.2 ± 0.1
Background	1127 ± 134	160 ± 23	82 ± 15
Data	1143	160	85
ZH (Predicted)	4.5 ± 0.4	1.8 ± 0.1	1.7 ± 0.1

with one loose SV tag and one JP tag (LJP), and the third contains events with just one tight SV tag (ST). These three regions are combined to search for ZH production. Table 1 shows the expected numbers of events for the signal and background processes, as well as the observed data.

5. Signal discrimination

In this analysis, we use a one-dimensional signal discriminant while maintaining the simultaneous separation of $t\bar{t}$ and Z + jets events from the ZH signal that was previously accomplished through a two-dimensional discriminant [9]. This method also further enhances signal discrimination by using two additional NNs in a multi-stage method, as described below.

We first train a NN signal discriminant, using several kinematic variables such as the dijet mass and E_T , to distinguish the signal-like (trained with ZH simulated events) and background-like (trained using a mixture of all background processes) events. Each data and simulated event is sent through the same signal discriminants, with a unique function optimized for 11 different Higgs mass hypotheses, defined in increments of $5 \text{ GeV}/c^2$ between 100 and $150 \text{ GeV}/c^2$.

The multi-stage method defines three samples (I, II, III) where events can enter the final distributions used for limit setting. The first step involves separating $t\bar{t}$ and Z + jets events. This is done using a NN function trained to separate these specific processes. A cut on the output of this discriminant is chosen to define a $t\bar{t}$ -enhanced sample (Sample I). Events which fail this cut and fall into Sample II or III are passed through a second NN function trained to separate b jets from charm and light flavor jets [28]. A cut on the output of this flavor separator function defines a sample containing mainly $Z + c\bar{c}$ and $Z + \text{LF}$ backgrounds (Sample II), and a region enriched in b jets (Sample III).

This multi-stage approach produces final output distributions with three samples enriched in various background processes, as seen in Fig. 1, where we add (0, 1, 2) to the signal discriminant output score for each event when the event falls in Sample (I, II, III) as described above. By enhancing the signal discrimination in this way, we increase the sensitivity of the analysis by $\sim 10\%$ over the technique used in Ref. [9]. We use these distributions to set limits on the ZH production cross section times $H \rightarrow b\bar{b}$ branching ratio.

6. Systematic uncertainties

We evaluate several systematic uncertainties on the background and signal events. A large source of systematic uncertainty arises from the cross section values used in the normalization of events: 40%, 10%, 6%, and 5%, for Z + heavy-flavor [29], $t\bar{t}$, diboson, and ZH simulated events, respectively. An uncertainty of (1, 2, 5)% is

³⁴ Forward ($|\eta| > 1.1$) electrons are exempt from this requirement.

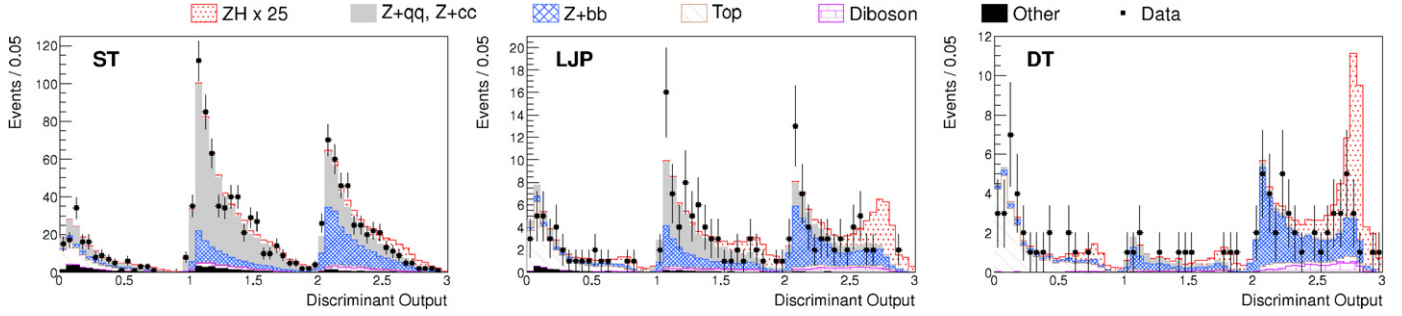


Fig. 1. Final discriminant output distributions for the three tag categories (ST, LJP, DT) used in this analysis. The distributions shown are for the discriminant trained on $m_H = 115 \text{ GeV}/c^2$ signal events. The ZH signal is shown, for $m_H = 115 \text{ GeV}/c^2$, and drawn scaled up by a factor of 25.

Table 2

Expected and observed 95% CL limits on the ZH production cross section times $H \rightarrow b\bar{b}$ branching ratio, relative to the expected standard model value, for each Higgs mass (in GeV/c^2) hypothesis.

m_H	100	105	110	115	120	125	130	135	140	145	150
Exp.	2.7	3.1	3.4	3.9	4.7	5.5	7.0	8.7	12	17	28
Obs.	2.8	3.3	4.4	4.8	5.4	4.9	6.6	7.3	10	14	22

applied to the (ST, LJP, DT) ZH samples after measuring changes in acceptance using simulated events with more or fewer particles radiated by the incoming and outgoing partons. The mistag prediction is measured using data, and carries a rate uncertainty of 14%, 27%, and 29%, for the ST, LJP, and DT tag categories, respectively. To account for differing b -jet identification efficiencies in data and simulated events, uncertainties of 5.2% (ST), 8.7% (LJP), and 10.4% (DT) are applied to the b -tagged samples. A 6% uncertainty is applied to simulated events, accounting for uncertainty in the measurement of integrated luminosity. The trigger model applied to simulated events requires a 5% normalization uncertainty. We also apply uncertainties on the lepton reconstruction and identification efficiency (1%) and lepton energy measurement (1.5%). For muons (electrons), we measure a 5% (50%) uncertainty on the normalization of the remaining background processes, based on differences in the rates of events containing same-charge and opposite-charge lepton pairs and in the rates of jets misidentified as electrons.

In addition, we account for sources of uncertainty that also include shape variations to account for the migration of events in the final signal discriminant distributions when fluctuating these shape-defining quantities within their uncertainties. These include uncertainties on the jet energies [30] as well as on the expected rate of Z + mistag events.

7. Results

Comparing the observed data to our background prediction including uncertainties, we do not find any evidence of a ZH signal. We set upper limits on the ZH production cross section times $H \rightarrow b\bar{b}$ branching ratio using a Bayesian algorithm [31], assuming a uniform prior on the signal rate. We do this by performing simulated experiments, each with a pseudo-dataset generated by randomly varying the normalizations of background processes within their respective statistical and systematic uncertainties, taking into account all background expectations in the absence of a signal. Each simulated experiment produces an upper limit on the ZH production cross section. The median of the 95% CL upper limits from the simulated experiments is taken to be the expected 95% CL upper limit of the analysis. We define the 1-sigma and 2-sigma deviations on the expected limit as the bounds which contain 68.3% and 95.5%, respectively, of the simulated experiment results. The observed data distribution is used to set the observed limit in a similar fashion. These limits are shown graphically, along with the

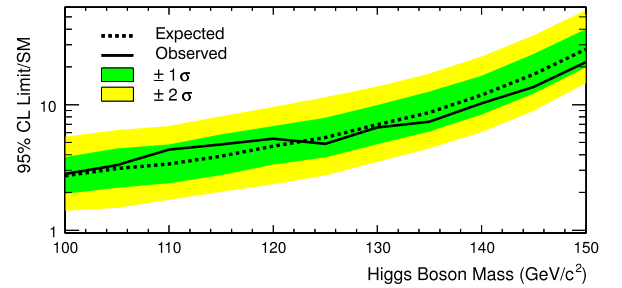


Fig. 2. Limits on the Higgs boson production cross section times the $H \rightarrow b\bar{b}$ branching ratio, given as a ratio to the standard model expected value.

1-sigma and 2-sigma ranges, in Fig. 2. Table 2 lists the expected and observed limits for each Higgs mass hypothesis considered in this analysis. We find that the observed limit is in good agreement with the expected limit for no signal, within the 1-sigma range across all Higgs mass hypotheses.

8. Conclusion

In conclusion, we have performed a search for the standard model Higgs boson in the process $ZH \rightarrow \ell^+\ell^-\bar{b}b$. The sensitivity of this analysis has improved due to several new multivariate techniques, including multivariate lepton identification, the use of NNs to obtain trigger efficiencies for simulated events, and a novel multi-stage discriminant approach used to enhance signal discrimination. We observe no significant excess and set an upper limit on the ZH production cross section times $H \rightarrow b\bar{b}$ branching ratio. We expect (observe) a limit of 3.9 (4.8) times the standard model predicted value, for a Higgs boson with mass $m_H = 115 \text{ GeV}/c^2$, at the 95% CL. The novel techniques presented here improve the sensitivity of the analysis by $\sim 25\%$ above the gain expected from the $\sim 85\%$ larger dataset.

Acknowledgements

We thank the Fermilab staff and the technical staffs of the participating institutions for their vital contributions. This work was supported by the U.S. Department of Energy and National Science Foundation; the Italian Istituto Nazionale di Fisica Nucleare; the Ministry of Education, Culture, Sports, Science and Technology of Japan; the Natural Sciences and Engineering Research

Council of Canada; the National Science Council of the Republic of China; the Swiss National Science Foundation; the A.P. Sloan Foundation; the Bundesministerium für Bildung und Forschung, Germany; the Korean World Class University Program, the National Research Foundation of Korea; the Science and Technology Facilities Council and the Royal Society, UK; the Russian Foundation for Basic Research; the Ministerio de Ciencia e Innovación, and Programa Consolider-Ingenio 2010, Spain; the Slovak R&D Agency; the Academy of Finland; and the Australian Research Council (ARC).

References

- [1] P.W. Higgs, Phys. Rev. Lett. 13 (1964) 508.
- [2] F. Englert, R. Brout, Phys. Rev. Lett. 13 (1964) 321.
- [3] G.S. Guralnik, C.R. Hagen, T.W.B. Kibble, Phys. Rev. Lett. 13 (1964) 585.
- [4] R. Barate, et al., LEP Working Group, Phys. Lett. B 565 (2003) 61.
- [5] CDF, D0 Collaborations, Tevatron New Phenomena, Higgs Working Group, arXiv:1107.5518, 2011, FERMILAB-CONF-11-354-E.
- [6] G. Aad, et al., ATLAS Collaboration, Phys. Lett. B 710 (2012) 49.
- [7] S. Chatrchyan, et al., CMS Collaboration, Phys. Lett. B 710 (2012) 26.
- [8] A. Djouadi, J. Kalinowski, M. Spira, Comput. Phys. Commun. 108 (1998) 56.
- [9] T. Aaltonen, et al., CDF Collaboration, Phys. Rev. Lett. 105 (2010) 251802.
- [10] V.M. Abazov, et al., D0 Collaboration, Phys. Rev. Lett. 105 (2010) 251801.
- [11] S. Lockwitz, Ph.D. thesis, Yale University, 2011, FERMILAB-THESIS-2012-02.
- [12] J. Pilot, PhD thesis, Ohio State University, 2011, FERMILAB-THESIS-2011-42.
- [13] D. Acosta, et al., CDF Collaboration, Phys. Rev. D 71 (2005) 052003.
- [14] A. Hocker, et al., PoS ACAT (2007) 040.
- [15] L. Balka, et al., Nucl. Instrum. Methods 267 (1988) 272.
- [16] M. Albrow, et al., Nucl. Instrum. Methods 480 (2002) 524.
- [17] A. Abulencia, et al., CDF Collaboration, J. Phys. G 34 (2007) 2457.
- [18] E. Thomson, et al., IEEE Trans. Nucl. Sci. 49 (2002) 1063.
- [19] A. Bhatti, et al., IEEE Trans. Nucl. Sci. 56 (2009) 1685.
- [20] G.C. Blazey, B.L. Flaugher, Annu. Rev. Nucl. Part. Sci. 49 (1999) 633.
- [21] M.L. Mangano, M. Moretti, F. Piccinini, R. Pittau, A.D. Polosa, J. High Energy Phys. 0307 (2003) 001.
- [22] T. Sjostrand, S. Mrenna, P.Z. Skands, J. High Energy Phys. 0605 (2006) 026.
- [23] F. Febres Cordero, L. Reina, D. Wackerroth, Phys. Rev. D 78 (2008) 074014.
- [24] J.M. Campbell, R. Ellis, Phys. Rev. D 60 (1999) 113006.
- [25] U. Langenfeld, S. Moch, P. Uwer, Phys. Rev. D 80 (2009) 054009.
- [26] D. Acosta, et al., CDF Collaboration, Phys. Rev. D 71 (2005) 052003.
- [27] A. Abulencia, et al., CDF Collaboration, Phys. Rev. D 74 (2006) 072006.
- [28] S. Richter, PhD thesis, Karlsruhe Institute of Technology, 2007, FERMILAB-THESIS-2007-35.
- [29] A. Abulencia, et al., CDF Collaboration, Phys. Rev. D 74 (2006) 032008.
- [30] A. Bhatti, et al., Nucl. Instrum. Methods A 566 (2006) 375.
- [31] K. Nakamura, et al., Particle Data Group, J. Phys. G 37 (2010).